ACS APPLIED MATERIALS & INTERFACES

Research Article

www.acsami.org

High Tumor Penetration of Paclitaxel Loaded pH Sensitive Cleavable Liposomes by Depletion of Tumor Collagen I in Breast Cancer

Li Zhang, Yang Wang, Yuting Yang, Yayuan Liu, Shaobo Ruan, Qianyu Zhang, Xiaowei Tai, Jiantao Chen, Tai Xia, Yue Qiu, Huile Gao, and Qin He*

Key Laboratory of Drug Targeting and Drug Delivery Systems, West China School of Pharmacy, Sichuan University, No. 17, Block 3, Southern Renmin Road, Chengdu, Sichuan 610041, China

Supporting Information

ABSTRACT: The network of collagen I in tumors could prevent the penetration of drugs loaded in nanoparticles, and this would lead to impaired antitumor efficacy. In this study, free losartan (an angiotensin inhibitor) was injected before treatment to reduce the level of collagen I, which could facilitate the penetration of nanoparticles. Then the pH-sensitive cleavable liposomes (Cl-Lip) were injected subsequently to exert the antitumor effect. The Cl-Lip was constituted by PEG_{5K}-Hydrazone-PE and DSPE-PEG_{2K}-R8. When the Cl-Lip reached to the tumor site by the enhanced permeability and retention (EPR) effect, PEG_{5K}-Hydrazone-PE was hydrolyzed from the Cl-Lip under the low extra-cellular pH conditions of tumors, then the R8 peptide was exposed, and finally liposomes could be internalized into tumor cells by the mediation of R8 peptide. *In vitro* experiments showed both the cellular uptake of Cl-Lip by 4T1 cells and cytotoxicity of paclitaxel loaded Cl-Lip (PTX-Cl-Lip) were pH sensitive. *In vivo* experiments showed the Cl-Lip had a good tumor targeting ability. After depletion of collagen I, Cl-Lip could penetrate into the deep place of tumors, the tumor accumulation of Cl-Lip was further increased by 22.0%, and the oxygen distributed in tumor tissues was also enhanced. The antitumor study indicated free losartan in combination with PTX-Cl-Lip (59.8%) was more effective than injection with PTX-Cl-Lip only (37.8%) in 4T1 tumor bearing mice. All results suggested that depletion of collagen I by losartan dramatically increased the penetration of PTX-Cl-Lip and combination of free losartan and PTX-CL-Lip could lead to better antitumor efficacy of chemical drugs. Thus, the combination strategy might be a promising tactic for better treatment of solid tumors with a high level of collagen I.

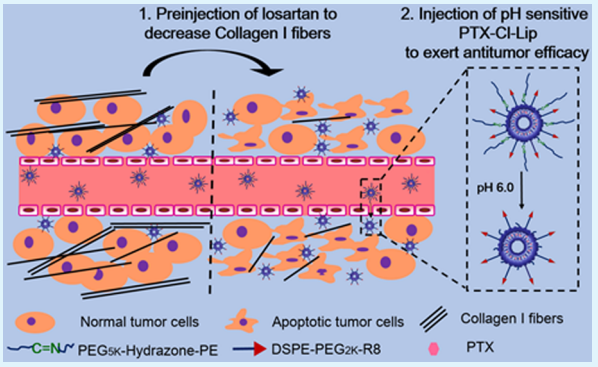

KEYWORDS: *drug delivery, losartan, drug penetration, pH-sensitive, cleavable PEG*

1. INTRODUCTION

Breast cancer was one of the most prevalent cancers among females.[1,2] A vital challenge of chemotherapy for breast cancer was to deliver drugs effectively into tumor tissues.[3,4] Nanoparticles had emerged as a valid drug carrier for cancer therapy, which could enhance the intratumoral accumulation of the payloads in nanoparticles and reduce the toxic side effects of small-molecule drugs.[5,6]

Although we could take advantage of the enhanced permeability and retention (EPR) effect to deliver nanoparticles to the tumor area,[7,8] the extracellular matrix (ECM) in tumors still hampered the penetration of nanoparticles, especially the network of collagen.[9] These collagen constituted up to 90% of ECM and was widespread in breast cancers and pancreatic cancers.[10] There were nearly 28 types of collagen being identified. Apart from collagen IV which provided structural support to organs and tissues, collagen I could construct a network between tumor cells.[11] The collagen I linked to tumor cells directly through the cell matrix and indirectly through cell−cell reactions. With the progression of tumors, the collagen I fibers straightened, bundled, and aligned. When the nanoparticles and oxygen reached to the tumor area, the collagen I fibers could prevent them from getting in touch with the tumor cells distributed in the deep sites of tumors. Therefore, the collagen I network could be an intrinsic transportation barrier to the functional nanoparticles and oxygen.[9,12] Strategies to decrease the level of collagen I before treatment could improve the penetration of nanoparticles and oxygen in tumors.

As an angiotensin inhibitor, losartan had high safety and low cost. More importantly, losartan could deplete collagen I in collagen-rich tumors including breast cancer and pancreatic cancer. In addition, losartan would not promote the tumor growth at a low dosage.[10,13] Thus, losartan might be a promising agent which was injected before the treatment to overcome the drawback of the tumor microenvironment. By this way, the high penetration of drugs and oxygen distribution in tumor tissues could be achieved.

Received: February 14, 2015
Accepted: April 7, 2015
Published: April 7, 2015

DOI: 10.1021/acsami.5b01473
ACS Appl. Mater. Interfaces 2015, 7, 9691−9701

After the modification of the tumor microenvironment, it was necessary to effectively transport the drugs to tumors. If we could establish a system with high tumor targeting ability and high internalization ability, the "better" tumor environment after depletion of collagen I could be made full use of and the desired antitumor efficacy could be obtained. So researchers modified the traditional PEG nanoparticles by many methods to achieve these two aims. Cell-penetrating peptides (CPPs) had been utilized for the superior ability to be taken up by tumor cells, but the *in vivo* application was limited for the poor selectivity of themselves.[14] To overcome this bottleneck, cleavable PEG with enzyme-sensitivity,[15] pH-sensitivity,[16] or reduction-sensitivity[17] was widely used in drug delivery systems.

Here we constructed an intelligent pH sensitive cleavable liposomal drug delivery system (Cl-Lip) by utilizing the low extracellular pH of tumors (Scheme 1).[18] It consisted of a short PEG attached by R8 peptide and a long pH-sensitive PEG derivative. R8 peptide was selected to enhance the cellular uptake of liposomes by tumor cells.[19] The long pH-sensitive PEG derivative was synthesized to overcome the nonselectivity of R8 peptide, and it was linked by a hydrazone bond. The hydrazone bond was selected because of the high pH sensitivity of the bond itself.[20,21] R8 peptide was shielded in blood circulation, when the liposomes accumulated to tumors by the EPR effect, R8 peptide could be exposed by the hydrolysis of PEG_{5K}-Hydrazone-PE under the low extracellular pH of tumors, then the liposomes internalized into the tumor cells by mediation of R8 peptide. Through this method, the drug delivery system owned a high tumor targeting ability and cellular internalization ability at the tumor area. Meanwhile, paclitaxel (PTX) was applied as a model drug loaded in the liposomes to avoid the toxicity of Cremophor EL/ethanol and serious side effects such as neurotoxicity and hypersensitivity reactions of free PTX.[22−24]

In summary, in this study, free losartan was administered before treatment, after the collagen I was significantly depleted by losartan, the pH sensitive liposomes (PTX-Cl-Lip) was subsequently injected (Scheme 1). We hoped that by the depletion of collagen I, the PTX-Cl-Lip could penetrate deeply into tumors and more PTX loaded in liposomes could accumulate in tumors. As a result, the PTX-Cl-Lip could exert a higher antitumor efficacy compare to the monotherapy.

Scheme 1. Schematic Illustration about the Effect of Losartan and the pH Sensitive Liposomes (PTX-Cl-Lip) in Tumor Area

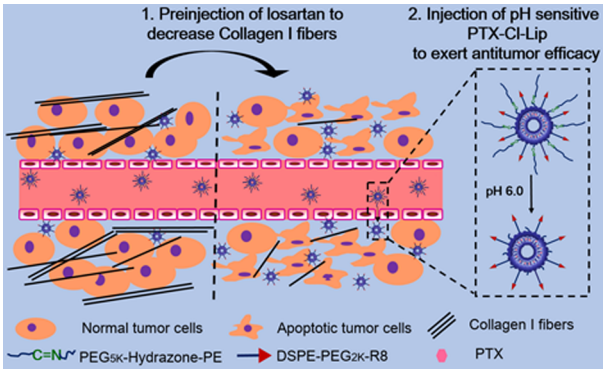

The combination strategy not only relieved the intrinsic weakness of the tumor microenvironment but also took advantage of passive targeting. At the same time, it could also avoid poor selectivity of CPPs and utilize the high internalization of CPPs. The prompt agent we used (losartan) was cheap and safe, and the drug delivery system we utilized had higher cellular internalization ability than the PEGlyation systems. Additionally, this combination strategy could noticeably enhance the antitumor efficacy to solid tumors with a high level of collagen I, and it hadn't been reported before. In our study, 4T1 cells were selected for high expression of collagen I.[13] The strategy was evaluated by the pH-sensitivity of the PTX-Cl-Lip, the level of collagen after injection of free losartan, the tumor distribution of liposomes with preinjection of free losartan, and antitumor efficacy of free losartan in combination with PTX-Cl-Lip.

2. MATERIALS AND METHODS

2.1. Materials. Methoxy (Polyethylene glysol)-5000 propionaldehyde (PEG_{5K}-CHO) was purchased from Jenkem Technology Co. Ltd. (Beijing, China). 3-(2-Pyridyldithio) propionyl hydrazide (PDPH) was purchased from Thermo Fisher Scientific Inc. (Waltham, MA). 1,2-Dipalmitoyl-*sn*-glycero-3-phosphothioethanol (PE-SH), 1,2-distearoyl-*sn*-glycero-3-phosphoethalamine-*N*-[methoxy(polyethylene glycol)-2000] (DSPE-PEG_{2K}-OMe), 1,2-distearoyl-*sn*-glycero-3-phosphoethalamine-*N*-[maleimide(polyethylene glycol)-2000] (DSPE-PEG_{2K}-Mal), and 1,2-dioleoyl-*sn*-glycero-3-phosphoethanolamine-*N*-(carboxyfluorescein) (CFPE) were purchased from Avanti Polar Lipids (Alabaster, AL). Soybean phospholipid (SPC) was purchased from Shanghai Advanced Vehicle Technology Ltd. Co. (Shanghai, China). Cholesterol was purchased from Chengdu Kelong Chemical Company (Chengdu, China). R8 peptide with a terminal cysteine (Cys-RRRRRRRR) was purchased from Chengdu Kai Jie Biopharmaceutical Co. Ltd. (Chengdu, China). 1,1′-Dioctadecyl-3,3,3′,3′-tetramethylindodicarbocyanine and 4-chlorobenzenesulfonate salt (DiD) were purchased from Biotium (Hayward, CA). Paclitaxel (PTX) was purchased from AP Pharmaceutical Co. Ltd. (Chongqing, China). losartan was purchased from Meilun Biotech Co. Ltd. (Dalian, China). 4′-6-Diamidino-2-pheylindole (DAPI) and 3-(4,5-dimethylthiazol-2-yl)-2,5-diphenyltetrazolium bromide (MTT) were purchased from Beyotime Institute Biotechnology (Haimen, China). The Annexin V-FITC/PI apoptosis detection kit was purchased from KeyGEN Biotech (Chengdu, China). Rabbit HIF-alpha (HIF-α) antibody and CD34 antibody were purchased from Abcam (Cambridge, MA). Alexa Fluor488 donkey antirabbit IgG (H+L) was purchased from Jackson Immuno Research (West Grove, PA). Rabbit Collagen I antibody was purchased from Proteintech (Chicago, IL). Evans Blue was purchased from Baoxin Biotech (Chengdu, China). Cell culture plastic plates were purchased from Wuxi NEST Biotechnology Co. (Wuxi, China). Other chemicals were purchased from relevant commercial companies.

Female Balb/c mice were purchased from the West China Animal Center of Sichuan University (Chengdu, China). All animal procedures were carried out under the protocol approved by the Experiment Animal Administrative Committee of Sichuan University.

2.2. Synthesis of PEG_{5K}-Hydrazone-PE. The synthesis procedure of PEG_{5k}-Hydrazone-PE was carried out by a two-step procedure according to previous method with some modifications[25] (Figure S1 in the Supporting Information). For step 1, 50 mg (0.21 mmol) cross-linker PDPH and 228 mg (0.04 mmol) PEG_{5K}-CHO were dissolved in 2 mL of anhydrous chloroform with the ratio 1:5 (−CHO/−NH_2). The reaction mixture was stirred at room temperature for 48 h. The product PEG_{5K}-Hydrazone-PDP was obtained by ether-precipitation. The yield of the product was 90.2%. The unconverted reactant PDPH in ether solution was collected for the same reaction next time. For step 2, 250.2 mg (0.033 mmol) of PEG_{5K}-Hydrazone-PDP, 13.7 mg (0.013 mmol) of PE, and 36.9 μL (0.12 μmol) of TEA were dissolved in 2 mL of anhydrous chloroform with the ratio 2.5:1:0.1 (PEG_{5K}-Hydrazone-PDP/PE/TEA). After 24 h reaction at room temperature,

DOI: 10.1021/acsami.5b01473
ACS Appl. Mater. Interfaces 2015, 7, 9691−9701

the mixture was concentrated by a rotary evaporator and precipitated by dry ether overnight. The precipitation was dissolved in deionized water with pH 10.5 (1 M NaOH) to get the PEG_{5K}-Hydrazone-PE micelles. The unreacted PEG_{5K}-Hydrazone-PE and 2-SH Pyridine were separated by a CL-4B column. Then the purified micelles were freeze-dried to obtain the final product. The yield of the product was 70.1%. The structure and molecular weight of PEG_{5K}-Hydrazone-PE were confirmed by ^1H NMR and mass spectrometry.

2.3. Synthesis of DSPE-PEG_{2k}-R8. In total, 10.0 mg (3.39 μmol) of DSPE-PEG_{2K}-Mal was dissolved in 4 mL of dry chloroform, and 7.2 mg (5.01 μmol) of cys-R8 in 2 mL of dry methanol was added in the above solvent, then 2 μL of TEA was added in the mixture solvent and reacted for 24 h under nitrogen atmosphere. The mixture solvent was evaporated by a rotary evaporator. The residue was redissolved in chloroform and the solvent was evaporated with a rotary evaporator once again to acquire the purified product. The yields of the product was 79.7%. The product was validated by mass spectrometry.

2.4. Preparation of Liposomes. Three kinds of liposomes were prepared by the thin film hydration method. PEGylated liposomes (PEG-Lip) were prepared by cholesterol, SPC, and DSPE-PEG_{2K}-OMe at the molar ratio of 35:65:0.8. R8 modified liposomes (R8-Lip) were prepared by cholesterol, SPC, and DSPE-PEG_{2K}-R8 at the molar ratio of 35:65:0.8. PEG_{5K}-Hydrazone-PE and R8 peptide surface-modified liposomes (Cl-Lip) were prepared by cholesterol, SPC, DSPE-PEG_{2K}-R8, and PEG_{5K}-Hydrazone-PE at the molar ratio of 35:57:0.8:8. All liposomal compositions were dissolved in chloroform, and then chloroform was removed from the mixture by a rotary evaporator to form lipid films and the films were further kept in vacuum overnight. All films were hydrated with PBS (pH 8.0) at 37 °C. The hydrated fluid was sonicated at 4 °C for 100 s to form liposomes. The liposomes were preserved at 4 °C for more experiments. For CFPE, DiD, PTX loading, a certain concentration of these materials were dissolved separately in chloroform and mixed with liposomal compositions before forming lipid films.

2.5. Characterization of Liposomes. The mean size and zeta potential of PEG-Lip, R8-Lip, and Cl-Lip were determined using a Malvern Zetasizer Nano ZS90 (Malvern Instruments Ltd., U.K.). The morphology of Cl-Lip was observed by a transmission electron microscope (TEM) (JEM-100CX, JEOL, Japan). The entrapment efficiency of PTX loaded liposomes was measured by high-performance liquid chromatography (HPLC, Alltech).

The serum stability of liposomes was determined in 50% fetal bovine serum (FBS). Briefly, the liposomes were incubated with the same volume of fetal bovine serum at 37 °C with shaking of 75 rpm for 24 h. The transmittance of the samples was detected at different time points under 750 nm by a micro plate reader (Thermo Scientific Varioskan Flash).

The drug release of PTX-loaded liposomes was determined by the dialysis method. The drug-loaded liposomes were dispersed in 1 mL of PBS and sealed tightly in dialysis tubes (MW = 8000). Then the dialysis tubes were immersed in 40 mL of PBS containing 1% Tween-80 and incubated under 37 °C with shaking of 75 rpm for 48 h. A volume of 100 μL of release media was taken out and replaced with the same volume of fresh release media at predetermined time intervals. The concentration of released PTX was determined by HPLC.

2.6. In Vitro pH Sensitivity of PEG_{5k}-Hydrazone-PE. In total, 4.0 mg of PEG_{5K}-Hydrazone-PE was used to form 2 mL of micelles by the thin film hydration method. Then the micelles were divided into 4 equal volumes and added into 1.0 mL of PBS of different pH (pH 5.0, pH 6.0, pH 7.4, and pH 8.0), respectively. After incubation at 37 °C for different times, 100 μL of mixture was removed from the samples and replaced with the same volume of fresh PBS of different pH. Ultrafiltration was used to separate the PEG_{5K}-Hydrazone-PE micelles and free PEG_{5K}, and the molecular weight cutoff (MWCO) was set to 100 kDa. Free PEG_{5K} was determined by the procedure of Deng et al.[26] Briefly, 100 μL of free PEG_{5K} was diluted with distilled water to get the final PEG_{5K} concentration within the range of 0−10 μg/mL. To a 4 mL sample, 500 μL of 5% barium chloride solution and 250 μL of iodine solution were added into free PEG_{5K} solution. Then the mixture was allowed to incubate 15 min for color development at room temperature. The absorbance of the complex was detected at 536 nm by a UV spectrophotometer.

2.7. Cellular Uptake on 4T1 Cells. A volume of 0.1 mL of CFPE-labeled PEG-Lip and R8-Lip were preincubated in 0.9 mL of serum free culture media 1640 at pH 7.4 each for 4 h at 37 °C, respectively. The same volume CFPE-labeled Cl-Lip was preincubated in 0.9 mL of serum free culture media 1640 at pH 6.0 or pH 7.4 each for 4 h at 37 °C. After the preincubation, the mixture of liposomes and culture media had its pH raised back to pH 7.4. Then, the culture media containing liposomes was added to 4T1 cells until the final concentration of CFPE reached 2 μg/mL. After incubation with 4T1 cells for 2 h at 37 °C, the cells were washed with PBS three times, treated with 0.25% trypsin solution, and suspended in 0.4 mL of PBS. The fluorescence intensity of different liposomes treated cells was detected by a flow cytometer (Cytomics FC 500, Beckman Coulter, Miami, FL).

For qualitative study, after above CFPE-labeled liposomes incubated with 4T1 cells for 2 h, cells were washed three times with PBS and fixed by 4% paraformaldehyde at room temperature for 30 min. Finally, the nuclei were stained by DAPI for 5 min in the dark. All cells were observed under a confocal laser scanning microscope (FV1000, Olympus).

2.8. In Vitro Cytotoxicity Study. The cytotoxicity of blank liposomes, free losartan, free PTX, and PTX-loaded liposomes were evaluated by MTT assay.[27,28] Primarily, 4T1 cells were seeded into 96-well plates (3000 cells/well) and grew for 24 h. Then the cells were reacted with a series concentration of blank liposomes, free losartan, free PTX, and PTX-loaded liposomes, respectively. After 48 h, 20 μL of MTT solution (5 mg/mL) was added into each well and continued to incubate for another 4 h. The crystals formed were dissolved in 150 μL of DMSO, and the plates were read by a micro plate reader at 490 nm (Thermo Scientific Varioskan Flash).

2.9. In Vitro Apoptosis Study. The quantitative analysis of cell apoptosis was evaluated by Annexin V-FITC/PI staining, after 4T1 cells were incubated with different liposomes at the dose of 2 μg/mL for 24 h, the cells were rinsed by PBS three times, suspended in 500 μL of binding buffer, and stained with 5 μL of Annexin V-FITC and 5 μL of PI according to the protocols, after 15 min, the cells were measured by a flow cytometer (Cytomics FC 500, Beckman Coulter, Miami, FL).

2.10. Penetration of Evans Blue in Tumors. Evans Blue's penetration was regarded as a marker of tumor penetration ability according to a previous study.[29] Female Balb/c mice weighing around 18−20 g were chosen to establish tumor models, and 10^6 4T1 cells were injected into the left flank area of mice. Twenty four mice with 4T1 tumors were randomly divided into different groups. When the tumors reached to an average volume of 200 mm^3, the mice of each losartan group received different concentrations of losartan solution daily by intraperitioneal injection, and the saline group received an injection of an equal volume of saline every day as well. Two weeks later, Evans Blue was injected at the dose of 60 mg/kg and allowed the dye-albumin complex to penetrate into tumor tissues for 24 h, then the tumor bearing mice were anaesthetized and perfused with PBS to remove the Evans Blue−Albumin complex in the vascular lumen. Finally, the tumors were weighed, and Evans Blue was extracted by formamide for 72 h at 37 °C. The concentration of Evans Blue in tumor tissues was measured by a UV spectrophotometer at 621 nm.

2.11. Biodistribution Study. When the tumors grew to an average volume of 200 mm^3, the mice were randomly divided into 5 groups (Blank, PEG-Lip, R8-Lip, Cl-Lip, and free losartan plus Cl-Lip), the free losartan plus Cl-Lip group was treated with 40 mg/kg by peritoneal injection continuously each day for 2 weeks, while the other groups were injected with the same volume of saline at the same time. On the last day of treatment, the mice were injected with PBS or DiD-labeled liposomes at the dose of 25 μg DiD/kg via caudal vein. After 24 h, the mice were imaged with an IVI Spectrum system (Caliper, Hopkington, MA). Then the mice hearts were perfused and fixed, and the hearts, livers, spleens, lungs, and kidneys of these mice were collected and imaged with an IVI Spectrum system. All the separated

DOI: 10.1021/acsami.5b01473
ACS Appl. Mater. Interfaces 2015, 7, 9691−9701

Table 1. Particle Sizes and Zeta Potentials of Blank Liposomes and PTX Loaded Liposomes under pH 7.4 (n = 3)

	size (nm)	PDI	zeta potential (mV)	entrapment efficiency (%)
PEG-Lip	99.2 ± 0.5	0.180 ± 0.006	−4.71 ± 0.11	
R8-Lip	101.0 ± 1.2	0.241 ± 0.008	0.48 ± 0.07	
CL-Lip	100.0 ± 7.7	0.190 ± 0.017	−4.36 ± 0.24	
PTX-PEG-Lip	107.0 ± 7.2	0.192 ± 0.003	−4.92 ± 0.13	94.03 ± 1.96
PTX-R8-Lip	122.8 ± 4.2	0.231 ± 0.015	0.49 ± 0.09	89.90 ± 2.73
PTX-Cl-Lip	117.1 ± 2.1	0.220 ± 0.034	−4.69 ± 0.08	94.28 ± 1.40

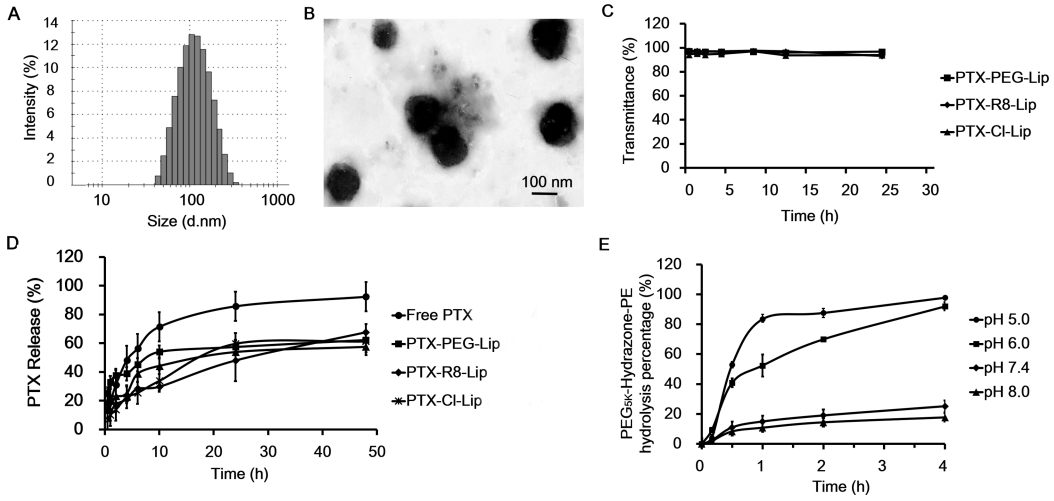

Figure 1. (A) Size distribution graph of PTX-Cl-Lip. (B) Size image of PTX-Cl-Lip observed under transmission electron microscope. (C) Transmittance of different liposomes in 50% FBS (n = 3). (D) PTX release percentage of free PTX and different liposomes over 48 h (n = 3). (E) PEG_{5K}-Hydrazone-PE hydrolysis percentage in different pH conditions (n = 3).

tumors frozen sectioned at the thickness of 10 μm. The samples were stained by collagen I antibody, HIF-1α antibody, and CD34 antibody, respectively, and then all samples were stained with DAPI for 5 min. Finally, the samples were observed under a confocal laser scanning microscope (FV1000, Olympus).

2.12. Antitumor Efficacy. Mice bearing 4T1 tumor were randomly divided into eight treatment groups (n = 6) when the tumors reached to 100−200 mm^3, then the mice were injected with 40 mg/kg losartan or an equal volume of saline through the peritoneal cavity subsequently each day, and the mice were injected with saline, free PTX, or different PTX loaded liposomes via caudal vein at the dose of 5 mg/kg every 3 days (4 h after losartan injection). The body weight and tumor volume of these mice were measured every 2 days. On the 27th day of the therapy, the mice were sacrificed and the tumors were separated and washed with cold PBS. Then the tumors were weighed and photographed. Hematoxylin and eosin (HE) staining on the paraffin-embeded tumors was performed according to the standard protocols provided by the manufacturers.

2.13. Statistical Analysis. All data were displayed as mean ± SD. Statistical difference between two groups were performed by the Students t test. A P value <0.05 and <0.01 were considered indications of statistical difference and statistically significant difference, respectively.

3. RESULTS

3.1. Synthesis of Materials. The hydrazone bond of PEG_{5K}-Hydrazone-PE was formed by the reaction between the −CHO of PEG_{5K}-CHO and $-NH_2$ of PDPH. The result of ^1H NMR (300 MHz, $CDCl_3$) confirmed the structure of the PEG_{5K} derivative (Figure S2A in the Supporting Information). From Figure S2A in the Supporting Information, the signal peak at 3.65 ppm was the characteristic peak of PEG (methylene groups), the peaks at 1.25 ppm were the characteristic peaks of PE (methylene groups), and the formation of hydrazone bond was validated by the signal peak at 8.05 ppm. The mass spectrometry also confirmed the successful synthesis of PEG_{5K}-Hydrazone-PE (Figure S2B in the Supporting Information) (observed MW = 5790.18 Da, calculated MW = 5867.3 Da).

R8 was conjugated to DSPE-PEG_{2K}-Mal by the reaction between the cysteine residue of R8 and maleimide of DSPE-PEG_{5K}-Mal. The mass spectrometry demonstrated the successful synthesis of DSPE-PEG_{2K}-R8 (Figure S3 in the Supporting Information) (observed MW = 4113.66 Da, calculated MW = 4312.78 Da).

3.2. Characterization of Liposomes. The basic properties of liposomes were important to further studies. According to the result, the sizes of blank liposomes were around 100 nm, while after PTX was loaded, the size of these liposomes were about 120 nm. Nevertheless, the PDI of all liposomes was less than 0.30 (Table 1 and Figure 1A). These data illuminated the homogeneity of all liposomes, and PEG_{5K}-Hydrazone-PE had no significant influence on the size of Cl-Lip. Transmission electron microscope proved the size of the PTX-Cl-Lip was almost 120 nm and these liposomes were generally spheroids (Figure 1B).

The zeta potential of PEG-Lip was negative. However, the zeta potential of R8-Lip was positive, due to the positive charge of R8 peptide. After PEG_{5K}-Hydrazone-PE shielding, the zeta potential of Cl-Lip was approximate to that of PEG-Lip. This result showed the amount of PEG_{5K}-Hydrazone-PE of Cl-Lip was sufficient to shield R8 peptide. Meanwhile, all entrapment efficiciencies of PTX loaded liposomes were nearly 90%.

3.3. In Vitro Stability in 50% FBS and PTX Release of Liposome. The transmittance of these liposomes was all above 90% after 24 h incubation, indicating the liposomes were stable

DOI: 10.1021/acsami.5b01473
ACS Appl. Mater. Interfaces 2015, 7, 9691−9701

in the *in vivo*-mimicking condition (Figure 1C). From the drug release property of different liposomes (Figure 1D), free PTX exhibited a rapid release of drug in the media, while the liposomes displayed a temperate release rate. After 48 h, the percentages of PTX released in all liposomes were close to 60% and no statistical difference was obtained between these liposomes.

3.4. In Vitro pH Sensitivity of PEG_{5K}-Hydrazone-PE. We performed the hydrolysis assay in PBS of different pH conditions to determine the pH-sensitivity of PEG_{5K}-Hydrazone-PE. The hydrolysis percentage of PEG_{5K}-Hydrazone-PE was nearly to 20% in pH 7.4 or pH 8.0 after 4 h incubation, while the hydrolysis percentage dramatically increased up to 90% in pH 5.0 or pH 6.0 after 4 h incubation (Figure 1E). Therefore, the hydrazone bond in the PEG_{5K} derivative could remain relatively stable in pH 7.4 or pH 8.0, while almost totally hydrolyzed in pH 5.0 or pH 6.0 after 4 h, indicating the PEG_{5K}-Hydrazone-PE could shield R8 peptide in physiological conditions and expose it in mild acid tumor area. This result confirmed the pH sensitivity of the hydrazone linkage and was consistent with previous studies.[25]

3.5. In Vitro Cellular Uptake Study. To evaluate the pH sensitivity of Cl-Lip, cellular uptake study was applied in this study. As the flow cytometry detected (Figure 2A), the fluorescence intensity of PEG-Lip preincubated in pH 7.4 was comparable to Cl-Lip preincubated under pH 7.4, and both of them were at a low level, which suggested R8 peptide was shielded by the PEG_{5K} derivative in pH 7.4. However, the fluorescence intensity of Cl-Lip preincubated in pH 6.0 was 8.0-fold higher than that in pH 7.4 condition. Although the fluorescence intensity of Cl-Lip preincubated in pH 6.0 was lower than that of R8-Lip, the two groups still had no significant difference. This result manifested the PEG_{5K} derivative of Cl-Lip could be almost totally removed and R8 peptide was exposed in mild acid conditions. The cellular uptake confirmed the PEG_{5K} derivative was sensitive to distinct pH conditions. It presented agreeable shielding and deshielding performance over R8 peptide under different pH conditions. At the same time, the confocal images indicated the identical result (Figure 2B). Additionally, R8-Lip could not enter the cell nucleus, which was in consistent with previous studies.[30] Similarly, Cl-Lip in pH 6.0 and pH 7.4 could not enter the cell nucleus either. Since neither PEG-Lip nor R8-Lip was pH-sensitive, the cellular uptake of the two liposomes preincubated in pH 6.0 was not evaluated.

3.6. Cytotoxicity Study and Apoptosis Assay in Vitro. MTT assay was employed to estimate the cytotoxicity of PTX loaded liposomes and losartan. The cell viability was all above 85% after 4T1 cells culturing with different concentrations of blank liposomes for 48 h (Figure 3A). Therefore, the materials constituting liposomes did not show obvious cytotoxicity to 4T1 cells. However, the PTX loaded liposomes exerted cytotoxicity in various degrees (Figure 3B). Nearly 75% cells after treating with PTX-PEG-Lip and PTX-Cl-Lip preincubated in pH 7.4 still remained viable even at the PTX concentration of 16 μg/mL for 48 h. In contrast, the alive cells treated with free PTX preincubated at pH 7.4, PTX-R8-Lip preincubated in pH 7.4, and PTX-Cl-Lip preincubated in pH 6.0 remained at a low level under the same conditions. The IC_{50} of free PTX preincubated in pH 7.4, PTX-R8-Lip preincubated in pH 7.4, and PTX-Cl-Lip preincubated in pH 6.0 was 5.32 μg/mL, 6.99 μg/mL, and 7.95 μg/mL, respectively. Owing to the fact that free PTX could enter into tumor cells by passive diffusion, the

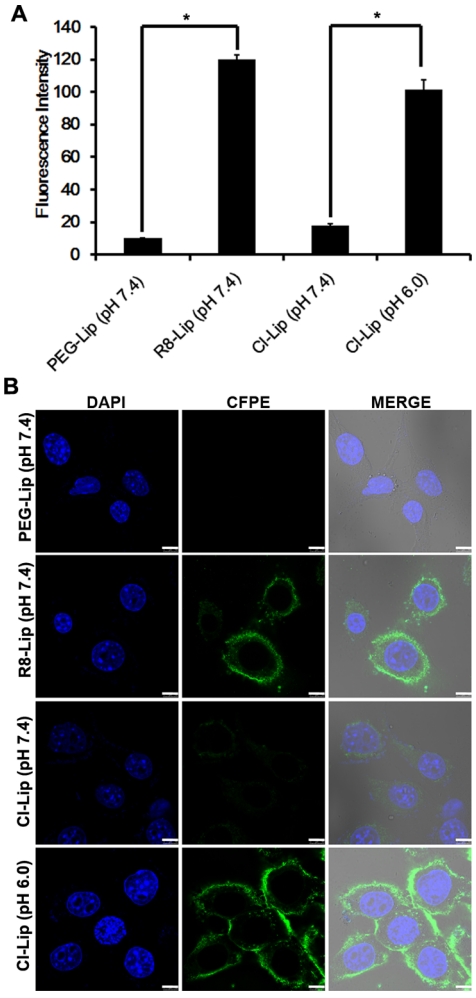

Figure 2. (A) Cellular uptake of liposomes with different preincubation on 4T1 cells detected by a flow cytometry (n = 3). * indicates $p < 0.05$. (B) Confocal images of cellular uptake of liposomes with different preincubation on 4T1 cells. Scale bars represent 25 μm.

IC_{50} of free PTX preincubated in pH 7.4 was lower than other groups.[31] The result above revealed the cytotoxicity of PTX-Cl-Lip was pH-dependent. In addition, when the cells were treated with free losartan for 48 h, there were 90.7% cells still kept alive even at the concentration of 64 μg/mL, indicating losartan did not show evident cytotoxicity to the cells.

From Figure 3C, PTX-PEG-Lip and PTX-Cl-Lip preincubated in pH 7.4 showed equivalent apoptosis and a necrosis ratio at 11.0 ± 0.5% and 14.1 ± 0.4%, respectively. By contrast, free PTX preincubated at pH 7.4, PTX-R8-Lip preincubated at pH 7.4, and PTX-Cl-Lip preincubated at pH 6.0 had a higher apoptosis-inducing effect, and the percentages of apoptotic and necrotic cells were 16.3 ± 0.8%, 19.0 ± 0.1%, and 20.5 ± 0.5%, respectively. This indicated after the PEG_{5K} derivative of PTX-Cl-Lip hydrolyzed, the apoptotic and necrotic percentage of PTX-Cl-Lip was increased by 45.4%. Free losartan showed the lowest apoptotic and necrotic ratio among all the groups (5.1 ± 0.9%). This was consistent with the result of the MTT assay.

3.7. Evans Blue Penetration Study. Evans Blue was a cationic dye which could spontaneously bind to serum albumin (negative charged) in blood circulation to form dye-albumin via electrostatic interaction. Since the formed dye-albumin were macromolecules, when the dye-albumin circulated to a tumor area by EPR effect, the dye-albumin could penetrate into

DOI: 10.1021/acsami.5b01473
ACS Appl. Mater. Interfaces 2015, 7, 9691−9701

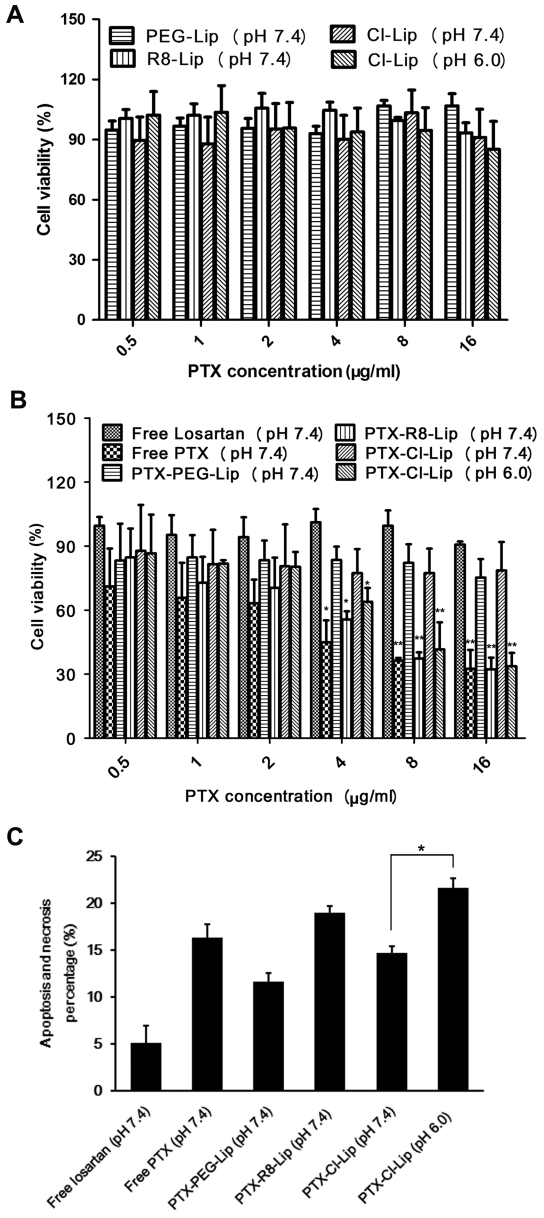

Figure 3. (A) Cytotoxicity study of blank liposomes preincubated in different pH conditions on 4T1 cells (n = 3). Horizontal coordinate represents corresponding PTX concentrations of blank vehicles. (B) The cytotoxicity study of free losartan, free PTX, and PTX loaded liposomes preincubated in different pH conditions on 4T1 cells (n = 3). Every concentration of losartan was 4 times PTX. * and ** indicate $p < 0.05$ and $p < 0.01$ versus the PTX-PEG-Lip group, respectively. (C) Percentage of apoptotic and necrotic 4T1 cells after treatment with all of the above preparations (n = 3). * indicates $p < 0.05$.

tumors. The penetration of Evans Blue in tumors could generally evaluate the penetration property of tumors.[32,33] According to Figure 4, compared to the saline group, injection of losartan at 10−40 mg/kg for 1 week did not significant enhance the penetration of Evans Blue in tumor tissues. However, after injection of losartan at 40 mg/kg for 2 weeks, the penetration of Evans Blue in tumor tissues was increased by 21.0%, and other losartan dosage of losartan injection for 2 weeks did not significantly affect the penetration of Evans Blue in tumor tissue in our study. This result indicated that with the preinjection of losartan at 40 mg/kg for 2 weeks, the drug penetration in tumors might be increased. Therefore,

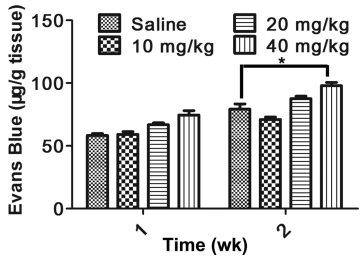

Figure 4. Effect of losartan with different dosages and treatment schedules on Evans Blue's penetration in tumors (n = 3). * indicates $p < 0.05$.

preinjection of losartan at 40 mg/kg for 2 weeks was selected in our further study.

3.8. In Vivo Image and Distribution Study. 4T1 tumor bearing Babl/c mice were used to estimate the tumor distribution of liposomes and the possible role of losartan in tumor treatment. From the *in vivo* and *ex vivo* images (Figure 5A,B), the fluorescence signal in tumor tissues of the Cl-Lip group was stronger than that of the PEG-Lip and R8-Lip group. It was 1.44-fold as the PEG-Lip group and 2.54-fold as the R8-Lip group from the semiquantitative result of the *ex vivo* images

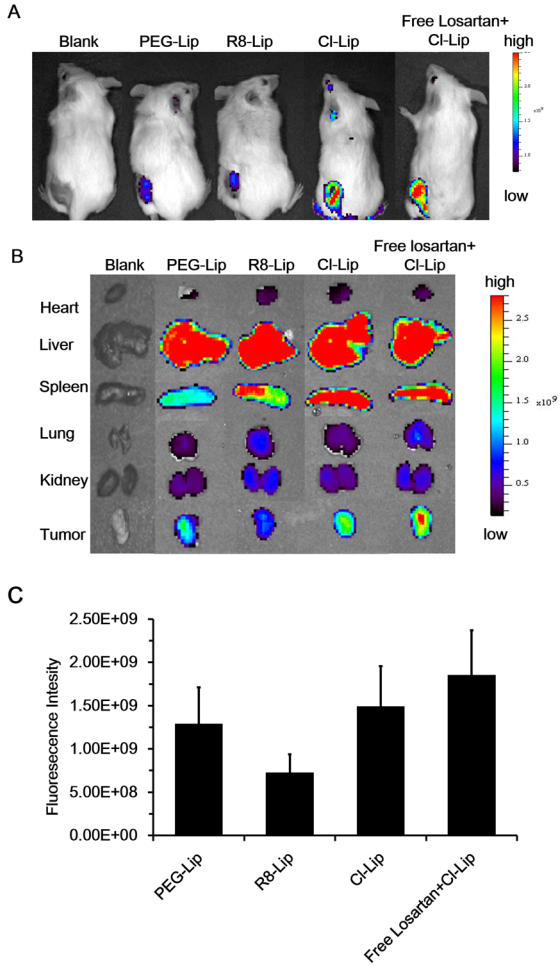

Figure 5. (A) *In vivo* images of 4T1 tumor bearing Babl/c mice with treatment of different preparations. (B) *Ex vivo* images about the distribution of DiD labeled liposomes in different organs. (C) Semiqualitative study of fluorescence intensity in tumors from the *ex vivo* images.

DOI: 10.1021/acsami.5b01473
ACS Appl. Mater. Interfaces 2015, 7, 9691−9701

(Figure 5C). More importantly, when the mice were injected with free losartan in combination with Cl-Lip, the fluorescence signal in the tumor region was further enhanced (Figure 5A,B), and the signal was 1.22-fold as the group only treated with Cl-Lip (Figure 5C). This result showed Cl-Lip had good tumor targeting ability and losartan could further enhance the accumulation of Cl-Lip in tumor tissues. The same result was also found in the confocal images (Figure 6). The *ex vivo* images clearly revealed the distribution of liposomes in livers and spleens was remarkably decreased in the Cl-Lip group and free losartan plus the Cl-Lip group compared to the R8-Lip group, especially the free losartan plus Cl-Lip group (Figure 5B).

Figure 6A displayed the group without injection of losartan and liposomes (Blank) had a high level of collagen I, demonstrating that the collagen I was widespread in 4T1 tumors. At the same time, the groups including the R8-Lip group, PEG-Lip group, and Cl-Lip group also had the same level of collagen I as the blank group, which showed injection of liposomes did not affect the level of collagen I. However, the collagen I level of Cl-Lip plus losartan was dramatically reduced compared to other groups. Therefore, the depletion of collagen was caused by injection of losartan.

In addition, the tumor tissues were also stained with CD34 antibody, which represented the location of blood vessels. It could be seen that after 24 h injection of DiD labeled liposomes, although the fluorescence signal of Cl-Lip was higher than that of PEG-Lip and R8-Lip, the Cl-Lip still located in or around the blood vessels. While the group with injection of losartan in advance showed that more much liposomes could accumulate in tumor sites than other groups and the liposomes in this group could penetrate much farther from the blood vessels in comparison with other groups. Hence, the injection of losartan in advance not only could increase the tumor accumulation of liposomes but also could lead to deep penetration of liposomes.

Since collagen I in tumor tissues also led to insufficient transportation of oxygen in the tumor area,[10,13] HIF-1α (a symbol of oxygen content of the organism) in tumor tissues was also labeled in our studies.[34] Figure 6C displayed the group with injection of losartan in advance had a lower HIF-1α level than other groups, which meant this group had high oxygen distribution intensity than others. As a consequence, losartan could be a promoter factor in delivering liposomes and oxygen to tumor tissues by decreasing the collagen I.

3.9. In Vivo Antitumor Efficacy. The pharmacological effect of different preparations was carried out on 4T1 tumor bearing mice. From Figure 7A, it could be seen the average tumor volume of the losartan group had no significant difference with the saline group. The result pointed out losartan at the dosage of 40 mg/kg for 2 weeks did not affect the growth rate of tumors. At the same time, the free PTX and combination of the two free drug did not show obvious antitumor efficacy. Although PTX-Cl-Lip improved the antitumor efficacy (with the tumor growth inhibition of 37.8%) to some extent, it was still lower than the combination of free losartan and PTX-Cl-Lip (with the tumor growth inhibition of 59.8%) (Figure 7A,C). Meanwhile, other groups did not show evident tumor inhibition ability. When the treatment procedure ended, the average tumor weight of the Saline group, Free Losartan group, Free PTX group, Free losartan + Free PTX group, PTX-PEG-Lip group, and PTX-R8-Lip group had no significant difference, all the average tumor

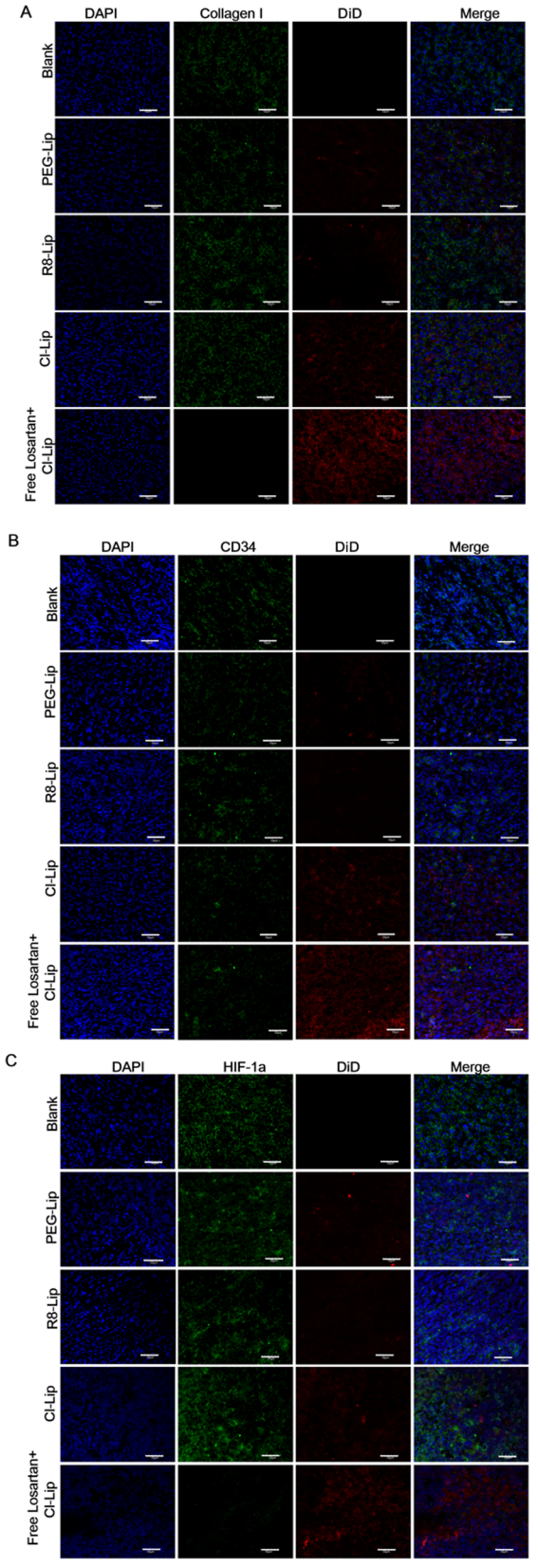

Figure 6. Confocal images of tumor tissue from 4T1 bearing mice injected by DiD labeled liposomes. (A) DAPI (blue), Collagen I (green), and DiD labeled liposomes (red). (B) DAPI (blue), CD34 (green), and DiD labeled liposomes (red). (C). DAPI (blue), HIF-1α (green), and DiD labeled liposomes (red). Scale bars represent 50 μm.

DOI: 10.1021/acsami.5b01473
ACS Appl. Mater. Interfaces 2015, 7, 9691−9701

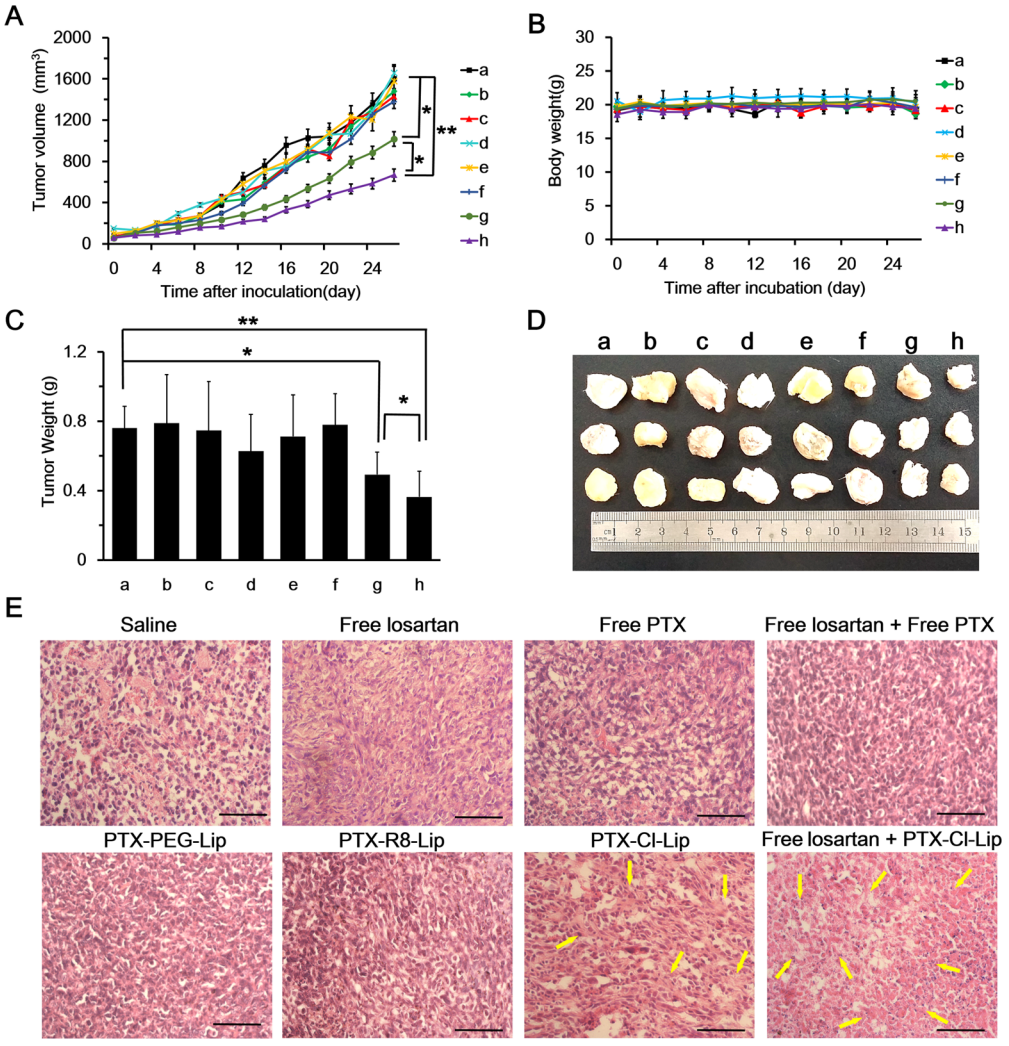

Figure 7. Antitumor efficacy of different preparations on 4T1 tumor bearing Balb/c mice. (A) Tumor growth curves of mice receiving different preparations (n = 6). (B) Body weight variations of mice during the treatment (n = 6). (C) Weights of extracted tumors at the end of the treatment procedure (n = 6). (D) Image of typical tumors at the end of the treatment procedure. In the above graphs, * and ** indicate $p < 0.05$ and $p < 0.01$, respectively. In all of the above groups, (a) Saline, (b) Free losartan, (c) Free PTX, (d) Free losartan + Free PTX, (e) PTX-PEG-Lip, (f) PTX-R8-Lip, (g) PTX-Cl-Lip, (h) Free losartan + PTX-Cl-Lip. (E) HE staining of tumors after treatment. Yellow arrows represent advanced cell apoptosis and necrosis in tumors. Scale bars represent 50 μm.

weight of these groups remained at a high level. By comparison, the average tumor weight of the PTX-Cl-Lip group and the free losartan plus PTX-Cl-Lip group decreased to 34.7% and 54.3%, respectively, compared to the Saline group (Figure 7C). The photograph of the typical tumors at the end of the therapy offered an intuitive proof of the remarkable antitumor efficacy of free losartan plus PTX-Cl-Lip (Figure 7D). When the therapy process ended, the body weights of all mice were around 20 g, indicating the high safety of losartan and the liposomes (Figure 7B). After the tumors were stained with HE, the free losartan plus PTX-Cl-Lip group generated more apoptotic and necrotic cells than other groups (pointed by yellow arrows) (Figure 7E).

4. DISCUSSION

Although the EPR effect could make the nanoparticles effectively accumulate in tumor sites, the intrinsic barriers seriously impaired the drug penetration in tumors, and this drawback significantly affected the antitumor efficacy of nanoparticles. Thus, it was important to deplete these intrinsic barriers including abnormal and high density of collagen I.[35] It could be predicted that the more nanoparticles penetrated into tumor cells and the higher possibility that nanoparticles penetrated deeply into tumors, the better antitumor efficacy could be obtained. Since the cancer stem cells could regenerate the tumor after therapy and existed in the deep region of the tumors,[36] the nanoparticles penetrated into the deep region of tumors might also cause the necrosis of cancer stem cells and prevent the regeneration of tumors.

On the basis of the characterization of the tumor targeting ability of nanoparticles and the intrinsic barriers of the tumor microenvironment, there were studies demonstrating combination therapy consisting of administration of one preparation to modify the tumor microenvironment and followed by administration of functional nanoparticles to exert the antitumor effect.[35,37] In our study, the intrinsic barrier, collagen I, was depleted by losartan to facilitate the penetration of functional nanoparticles, which had higher safety than others. What's more, according to previous studies, the functional nanoparticles were always traditional PEG nanoparticles and

DOI: 10.1021/acsami.5b01473
ACS Appl. Mater. Interfaces 2015, 7, 9691−9701

the poor internalization of PEG significantly impaired the antitumor efficacy. In order to obtain the maximum antitumor efficacy after depletion of collagen I, there was much room for the PEG nanoparticles to improve.

Thus, in the first place, we constructed a pH sensitive cleavable drug delivery system (Cl-Lip) which owned both high tumor targeting ability and high internalization ability at tumor sites. To the Cl-Lip we designed, the long PEG at the molecule weight of 5000 was used for shielding the R8 peptide and the short PEG at the molecule weight of 2000 attaching the R8 peptide was chosen according to our previous studies.[38,39] This was because the liposomes modified with these two PEG with the molecular weight and the ratio we predetermined could provide the highest mask effect on the R8 peptide. It was an improvement compared to previous studies.[25]

It was beneficial for the Cl-Lip for passive targeting having an average size around 117.1 nm, as the liposomes with an average diameter of 100−200 nm could effectively accumulate in tumors.[40] The zeta potential of R8-Lip was the result of the high pH of PBS (pH 8.0) used to hydrate R8-Lip. The PBS under pH 8.0 was utilized in order to reduce the percentage of hydrolyzed PEG_{5K}-Hydrazone-PE during the procedure of storage. Nevertheless, Cl-Lip still had a higher negative charge than that of R8-Lip, so the potential difference of the two kinds of liposomes could demonstrate the desirable shielding effect of PEG_{5K}-Hydrazone-PE. Moreover, the positive charge of R8 would increase the instability of liposomes *in vivo*,[41] so the negative zeta potential of Cl-Lip also indicated the increased stability of Cl-Lip *in vivo*. The high stability of Cl-Lip was also verified by the serum stability study (Table 1 and Figure 2C). In addition, the moderate PTX release of the PTX loaded liposomes implied the drugs in liposomes could efficiently reach to the tumor area even after 48 h (Figure 2D). These basic characteristics of PTX-Cl-Lip laid the foundation for further studies.

In vitro studies showed the hydrolysis of the PEG derivative was pH-responsive (Figure 2E). It was because of the pH sensitivity of the PEG-Hydrazone-PE itself. Liposomes preincubated with 1640 culture medium of different pH conditions was to hydrolyze the PEG_{5K}-Hydrazone-PE modified on the surface of Cl-Lip under *in vitro* conditions. According to the *in vitro* hydrolysis percentage of PEG_{5K}-Hydrazone-PE, the cellular uptake intensity under different conditions could be evaluated. The time period of 4 h was chosen because nearly 90% of PEG_{5K}-Hydrazone-PE could be hydrolyzed in pH 6.0 and the hydrolysis difference of PEG_{5K}-Hydrazone-PE between pH 6.0 and pH 7.4 was noticeable. After hydrolysis of PEG_{5K}-Hydrazone-PE, Cl-Lip was positive charged and it could benefit the interaction of a negatively charged cell membrane and the liposomes. It was all above factors that lead to the higher uptake of Cl-Lip in pH 6.0 than in pH 7.4 (Figure 3), which indicated the cellular uptake of Cl-Lip was pH-sensitive. The higher uptake of R8-Lip than Cl-Lip in pH 6.0 might be due to existing PEG_{5K}-Hydrazone-PE on the surface of Cl-Lip after 4 h preincubation. Since Cl-Lip internalized into cells via mediation of R8, the uptake mechanism of Cl-Lip was similar to that of R8-Lip. Previous studies showed the uptake of R8-Lip was dependent on many pathways, the two main ways were clathrin-mediated endocytosis and macropinocytosis-mediated endocytosis.[41] Therefore, the uptake of Cl-Lip in lower pH probably also depended on these two pathways.

From *in vivo* studies, the fluorescence intensity of Cl-Lip group in tumors was higher than that of PEG-Lip and R8-Lip group, demonstrating the Cl-Lip had high tumor targeting ability (Figures 6 and 7B). This was because the PEGylation of Cl-Lip was in physiological conditions. The PEG derivative in Cl-Lip could shield the R8 peptide and keep stable in such a microenvironment, and it could prolong the blood circulation time of liposomes as well.[42] Since the high density PEG of liposomes could lead to a "brush" formation of PEG, and this formation was more beneficial for reticuloendothelial system evasion than the liposomes with low PEG density,[41] the tumor targeting ability of Cl-Lip (8% PEG) was higher than that of PEG-Lip (0.8% PEG). The tumor targeting ability of R8-Lip was seriously limited by the poor selectivity and instability of R8 peptide. In the terms of PTX loaded liposomes, the poor antitumor efficacy of free PTX was the result of its poor tumor targeting ability. As to PTX-PEG-Lip, the undesired effect was because of the poor internalization ability and tumor targeting ability, while the damaged effect of PTX-R8-Lip was on account of poor tumor targeting ability. Since the dosage (5 mg/kg) we utilized was low and treatment schedule (every third day) was not frequent, these two factors might also be the reasons for the undesirable antitumor effect of free PTX, PTX-R8-Lip, and PTX-PEG-Lip. Because of the high tumor targeting ability of Cl-Lip and the high internalization ability of these liposomes in mild acid conditions, the tumor inhibition rate of PTX-Cl-Lip was higher than free PTX, PTX-PEG-Lip, and PTX-R8-Lip (Figure 7). All the results proved the PTX-Cl-Lip could shield R8 peptide in physiological conditions and expose it when liposomes accumulated to the tumor sites. Therefore, the PTX loaded in PTX-Cl-Lip could effectively accumulate in the tumor area to exert the pharmacological effect.

Before losartan was administrated *in vivo* with Cl-Lip, we tested the cytotoxicity of losartan to 4T1 cells. The result of MTT and apoptosis study showed nearly 90% cells were alive under all concentrations we set (Figure 4), confirming the high safety of losartan. Another issue we must pay attention to was the antihypertension effect of losartan. The dosage and treatment schedules of losartan should not lower the mean arterial blood pressure (MABP). Previous studies manifested losartan treatment at 20 mg/kg or 40 mg/kg for 2 weeks before tumor treatment would not lower the MABP in the mice.[10,13] Thus, the dose and dosing schedule of losartan in our study (40 mg/kg) had a minimal effect on blood pressure and maximum effect on depletion of collagen I. Then we verified the promotion effect of losartan in tumor penetration with Evans Blue. After we injected losartan at 40 mg/kg for 2 weeks, the penetration of Evans Blue in tumors was significantly enhanced compared to the saline group (Figure 5). The result showed losartan might facilitate the penetration of macromolecules and functional nanoparticles in tumors.

When free losartan was in combination with Cl-Lip, *in vivo* imaging showed the liposomes accumulated in tumors was remarkably increased compared to the mice with only injection of Cl-Lip, which had the highest fluorescence signal intensity among all groups (Figures 6 and 7). By the staining of collagen I, we found the injection of losartan could decrease the level of collagen I (Figure 7A), while other groups had high collagen I level. More importantly, after the intrinsic barrier of collagen I was weakened, the liposomes could distributed farther from the blood vessels compared to the groups without injection of losartan (Figure 7B). This result indicated that the Cl-Lip could penetrate into deep place of tumors by depletion of collagen I.

DOI: 10.1021/acsami.5b01473
ACS Appl. Mater. Interfaces 2015, 7, 9691−9701

So, in term of the high tumor accumulation of Cl-Lip after preadministration of losartan, it was all the factors combined including the high penetration of Cl-Lip by depletion of collagen I and high tumor targeting of Cl-Lip (Figure 6). Meanwhile, the decreased level of HIF-1α demonstrated the enhanced oxygen distribution intensity in tumors after injection of losartan (Figure 7C). Herein, the depletion of collagen I by losartan paved the way for the delivery of liposomes and oxygen into tumor tissues.

The studies of Jain et al. elucidated that losartan decreased the collagen I level in tumors by down-regulating the active transforming growth factor-β1 (TGF-β1).[10,43] Their studies also discovered that collagen fibers interacted with hyaluronan in a complex manner and both contributed to the accumulation of solid stress. Reduction of collagen I can also ease the compression of hyaluronan to tumor vessels.[13]

Consequently, because of the enhanced penetration of Cl-Lip after the depletion of collagen I by losartan, the passive tumor targeting of Cl-Lip and high internalization ability of Cl-Lip under the low extracellular pH of tumor sites, it was reasonable that the combination of losartan and PTX-Cl-Lip displayed the highest tumor inhibition rate than other groups. While the damaged effect of the combination of free PTX and free losartan was mainly due to the poor tumor growth inhibition ability of free PTX. With the depletion of collagen I by losartan, the dosage of PTX we used was reduced in comparison with other dosages such as 10 and 15 mg/kg.[44,45] Although there also were reports showing the losartan could attenuate the growth of tumors,[46] a similar result was not obtained in our studies. This might be due to the low dose of losartan we injected. In summary, only when depletion of collagen I by preadministration of losartan was in combination with an effective drug delivery system PTX-Cl-Lip could the best antitumor efficacy among the eight groups be achieved.

5. CONCLUSION

In this study, losartan was administered in advance to deplete collagen I so that the penetration of liposomes and distribution intensity of oxygen could be improved in 4T1 breast cancer. Meanwhile, the intelligent pH sensitive cleavable liposomal drug delivery system (PTX-Cl-Lip) consisted of PTX, R8 peptide, and a pH-sensitive PEG derivative and was successfully constructed. It possessed high accumulation and internalization ability in the tumor area. When losartan was in combination with PTX-Cl-Lip, the chemotherapy efficacy of PTX-Cl-Lip in 4T1 bearing mice was remarkably increased compared to PTX-Cl-Lip alone. Therefore, the reduction of collagen I by losartan to enhance the penetration of paclitaxel loaded cleavable pH-sensitive liposomes could be a promising strategy, which would bring about enhanced antitumor effect in breast cancer treatment.

■ ASSOCIATED CONTENT

Supporting Information

Synthetic route, ^{1}H NMR spectrum and mass spectrum of PEG_{5K}-Hz-PE and mass spectrum of DSPE-PEG_{2K}-R8. This material is available free of charge via the Internet at http://pubs.acs.org.

■ AUTHOR INFORMATION

Corresponding Author

*Phone/fax: +86-28-85502532. E-mail: qinhe@scu.edu.cn.

Notes

The authors declare no competing financial interest.

■ ACKNOWLEDGMENTS

The work was funded by the National Natural Science Foundation of China (Grant 81373337) and the National Basic Research Program of China (973 program, Grant 2013CB932504).

■ REFERENCES

(1) DeSantis, C. E.; Lin, C. C.; Mariotto, A. B.; Siegel, R. L.; Stein, K. D.; Kramer, J. L.; Alteri, R.; Robbins, A. S.; Jemal, A. Cancer Treatment and Survivorship Statistics, 2014. *Ca-Cancer J. Clin.* **2014**, *64*, 252−271.

(2) Crozier, J. A.; Swaika, A.; Moreno-Aspitia, A. Adjuvant Chemotherapy in Breast Cancer: To Use Or Not to Use, the Anthracyclines. *World J. Clin. Oncol.* **2014**, *5*, 529−538.

(3) Ferrari, M. Cancer Nanotechnology: Opportunities and Challenges. *Nat. Rev. Cancer* **2005**, *5*, 161−171.

(4) Jain, R. K.; Stylianopoulos, T. Delivering Nanomedicine to Solid Tumors. *Nat. Rev. Clin. Oncol.* **2010**, *7*, 653−664.

(5) Brannon-Peppas, L.; Blanchette, J. O. Nanoparticle and Targeted Systems for Cancer Therapy. *Adv. Drug Delivery Rev.* **2004**, *56*, 1649−1659.

(6) Lee, S. M.; Ahn, R. W.; Chen, F.; Fought, A. J.; O'Halloran, T. V.; Cryns, V. L.; Nguyen, S. T. Biological Evaluation of pH-responsive Polymer-Caged Nanobins for Breast Cancer Therapy. *ACS Nano* **2010**, *4*, 4971−4978.

(7) Maeda, H.; Nakamura, H.; Fang, J. The EPR Effect for Macromolecular Drug Delivery to Solid Tumors: Improvement of Tumor Uptake, Lowering of Systemic Toxicity, and Distinct Tumor Imaging in Vivo. *Adv. Drug Delivery Rev.* **2013**, *65*, 71−79.

(8) Shao, Y.; Shi, C.; Xu, G.; Guo, D.; Luo, J. Photo and Redox Dual Responsive Reversibly Cross-Linked Nanocarrier for Efficient Tumor-Targeted Drug Delivery. *ACS Appl. Mater. Interfaces* **2014**, *6*, 10381−10392.

(9) Provenzano, P. P.; Eliceiri, K. W.; Campbell, J. M.; Inman, D. R.; White, J. G.; Keely, P. J. Collagen Reorganization at the Tumor-Stromal Interface Facilitates Local Invasion. *BMC Med.* **2006**, *4*, 38.

(10) Diop-Frimpong, B.; Chauhan, V. P.; Krane, S.; Boucher, Y.; Jain, R. K. Losartan Inhibits Collagen I Synthesis and Improves the Distribution and Efficacy of Nanotherapeutics in Tumors. *Proc. Natl. Acad. Sci. U.S.A.* **2011**, *108*, 2909−2914.

(11) Fang, M.; Yuan, J.; Peng, C.; Li, Y. Collagen as a Double-Edged Sword in Tumor Progression. *Tumor Biol.* **2014**, *35*, 2871−2882.

(12) Netti, P. A.; Berk, D. A.; Swartz, M. A.; Grodzinsky, A. J.; Jain, R. K. Role of Extracellular Matrix Assembly in Interstitial Transport in Solid Tumors. *Cancer Res.* **2000**, *60*, 2497−2503.

(13) Chauhan, V. P.; Martin, J. D.; Liu, H.; Lacorre, D. A.; Jain, S. R.; Kozin, S. V.; Stylianopoulos, T.; Mousa, A. S.; Han, X.; Adstamongkonkul, P.; Popovic, Z.; Huang, P.; Bawendi, M. G.; Boucher, Y.; Jain, R. K. Angiotensin Inhibition Enhances Drug Delivery and Potentiates Chemotherapy by Decompressing Tumour Blood Vessels. *Nat. Commun.* **2013**, *4*, 2516.

(14) Gao, H.; Zhang, Q.; Yu, Z.; He, Q. Cell-Penetrating Peptide-Based Intelligent Liposomal Systems for Enhanced Drug Delivery. *Curr. Pharm. Biotechnol.* **2014**, *10*, 210−219.

(15) Zhu, L.; Wang, T.; Perche, F.; Taigind, A.; Torchilin, V. P. Enhanced Anticancer Activity of Nanopreparation Containing an MMP2-sensitive PEG-drug Conjugate and Cell-Penetrating Moiety. *Proc. Natl. Acad. Sci. U.S.A.* **2013**, *110*, 17047−17052.

(16) Nie, Y.; Gunther, M.; Gu, Z.; Wagner, E. Pyridylhydrazone-Based PEGylation for pH-reversible Lipopolyplex Shielding. *Biomaterials* **2011**, *32*, 858−869.

(17) Meng, F.; Hennink, W. E.; Zhong, Z. Reduction-Sensitive Polymers and Bioconjugates for Biomedical Applications. *Biomaterials* **2009**, *30*, 2180−2198.

DOI: 10.1021/acsami.5b01473
ACS Appl. Mater. Interfaces 2015, 7, 9691−9701

(18) Felber, A. E.; Dufresne, M. H.; Leroux, J. C. PH-sensitive Vesicles, Polymeric Micelles, and Nanospheres Prepared with Polycarboxylates. *Adv. Drug Delivery Rev.* **2012**, *64*, 979−992.
(19) Nakase, I.; Konishi, Y.; Ueda, M.; Saji, H.; Futaki, S. Accumulation of Arginine-Rich Cell-Penetrating Peptides in Tumors and the Potential for Anticancer Drug Delivery in Vivo. *J. Controlled Release* **2012**, *159*, 181−188.
(20) Chan, Y.; Bulmus, V.; Zareie, M. H.; Byrne, F. L.; Barner, L.; Kavallaris, M. Acid-Cleavable Polymeric Core-Shell Particles for Delivery of Hydrophobic Drugs. *J. Controlled Release* **2006**, *115*, 197−207.
(21) Zhou, Z.; Li, L.; Yang, Y.; Xu, X.; Huang, Y. Tumor Targeting by pH-sensitive, Biodegradable, Cross-Linked N-(2-hydroxypropyl) Methacrylamide Copolymer Micelles. *Biomaterials* **2014**, *35*, 6622−6635.
(22) Koudelka, S.; Turanek, J. Liposomal Paclitaxel Formulations. *J. Controlled Release* **2012**, *163*, 322−334.
(23) Liu, Y.; Fang, J.; Kim, Y. J.; Wong, M. K.; Wang, P. Codelivery of Doxorubicin and Paclitaxel by Cross-Linked Multilamellar Liposome Enables Synergistic Antitumor Activity. *Mol. Pharmaceutics* **2014**, *11*, 1651−1661.
(24) Liu, J.; Gaj, T.; Patterson, J. T.; Sirk, S. J.; Barbas, C. R. Cell-Penetrating Peptide-Mediated Delivery of TALEN Proteins Via Bioconjugation for Genome Engineering. *PLoS One* **2014**, *9*, e85755.
(25) Sawant, R. M.; Hurley, J. P.; Salmaso, S.; Kale, A.; Tolcheva, E.; Levchenko, T. S.; Torchilin, V. P. "SMART" Drug Delivery Systems: Double-Targeted pH-responsive Pharmaceutical Nanocarriers. *Bioconjugate Chem.* **2006**, *17*, 943−949.
(26) Xu, H.; Deng, Y.; Chen, D.; Hong, W.; Lu, Y.; Dong, X. Esterase-Catalyzed dePEGylation of pH-sensitive Vesicles Modified with Cleavable PEG-lipid Derivatives. *J. Controlled Release* **2008**, *130*, 238−245.
(27) Schroeder, B. R.; Ghare, M. I.; Bhattacharya, C.; Paul, R.; Yu, Z.; Zaleski, P. A.; Bozeman, T. C.; Rishel, M. J.; Hecht, S. M. The Disaccharide Moiety of Bleomycin Facilitates Uptake by Cancer Cells. *J. Am. Chem. Soc.* **2014**, *136*, 13641−13656.
(28) Raghavendra, G. M.; Jayaramudu, T.; Varaprasad, K.; Reddy, G. S. M.; Raju, K. M. Antibacterial Nanocomposite Hydrogels for Superior Biomedical Applications: A Facile Eco-Friendly Approach. *RSC Adv.* **2015**, 14351−14358.
(29) Warnick, R. E.; Fike, J. R.; Chan, P. H.; Anderson, D. K.; Ross, G. Y.; Gutin, P. H. Measurement of Vascular Permeability in Spinal Cord Using Evans Blue Spectrophotometry and Correction for Turbidity. *J. Neurosci. Methods* **1995**, *58*, 167−171.
(30) Liu, Y.; Ran, R.; Chen, J.; Kuang, Q.; Tang, J.; Mei, L.; Zhang, Q.; Gao, H.; Zhang, Z.; He, Q. Paclitaxel Loaded Liposomes Decorated with a Multifunctional Tandem Peptide for Glioma Targeting. *Biomaterials* **2014**, *35*, 4835−4847.
(31) Shao, K.; Ding, N.; Huang, S.; Ren, S.; Zhang, Y.; Kuang, Y.; Guo, Y.; Ma, H.; An, S.; Li, Y.; Jiang, C. Smart Nanodevice Combined Tumor-Specific Vector with Cellular Microenvironment-Triggered Property for Highly Effective Antiglioma Therapy. *ACS Nano* **2014**, *8*, 1191−1203.
(32) Wu, J.; Akaike, T.; Maeda, H. Modulation of Enhanced Vascular Permeability in Tumors by a Bradykinin Antagonist, a Cyclooxygenase Inhibitor, and a Nitric Oxide Scavenger. *Cancer Res.* **1998**, *58*, 159−165.
(33) Ogawara, K.; Un, K.; Minato, K.; Tanaka, K.; Higaki, K.; Kimura, T. Determinants for in Vivo Anti-Tumor Effects of PEG Liposomal Doxorubicin: Importance of Vascular Permeability within Tumors. *Int. J. Pharm.* **2008**, *359*, 234−240.
(34) Galanis, A.; Pappa, A.; Giannakakis, A.; Lanitis, E.; Dangaj, D.; Sandaltzopoulos, R. Reactive Oxygen Species and HIF-1 Signalling in Cancer. *Cancer Lett.* **2008**, *266*, 12−20.
(35) Kohli, A. G.; Kivimae, S.; Tiffany, M. R.; Szoka, F. C. Improving the Distribution of Doxil(R) in the Tumor Matrix by Depletion of Tumor Hyaluronan. *J. Controlled Release* **2014**, *191*, 105−114.
(36) Ju, C.; Mo, R.; Xue, J.; Zhang, L.; Zhao, Z.; Xue, L.; Ping, Q.; Zhang, C. Sequential Intra-Intercellular Nanoparticle Delivery System for Deep Tumor Penetration. *Angew. Chem., Int. Ed.* **2014**, *53*, 6253−6258.
(37) Fan, Y.; Du, W.; He, B.; Fu, F.; Yuan, L.; Wu, H.; Dai, W.; Zhang, H.; Wang, X.; Wang, J.; Zhang, X.; Zhang, Q. The Reduction of Tumor Interstitial Fluid Pressure by Liposomal Imatinib and its Effect On Combination Therapy with Liposomal Doxorubicin. *Biomaterials* **2013**, *34*, 2277−2288.
(38) Yuan, W.; Kuai, R.; Ran, R.; Fu, L.; Yang, Y.; Qin, Y.; Liu, Y.; Tang, J.; Fu, H.; Zhang, Q.; Yuan, M.; Zhang, Z.; Gao, F.; He, Q. Increased Delivery of Doxorubicin Into Tumor Cells Using Extracellularly Activated TAT Functionalized Liposomes: In Vitro and in Vivo Study. *J. Biomed. Nanotechnol.* **2014**, *10*, 1563−1573.
(39) Kuai, R.; Yuan, W.; Qin, Y.; Chen, H.; Tang, J.; Yuan, M.; Zhang, Z.; He, Q. Efficient Delivery of Payload Into Tumor Cells in a Controlled Manner by TAT and Thiolytic Cleavable PEG Co-Modified Liposomes. *Mol. Pharmaceutics* **2010**, *7*, 1816−1826.
(40) Hatakeyama, H.; Akita, H.; Harashima, H. A Multifunctional Envelope Type Nano Device (MEND) for Gene Delivery to Tumours Based On the EPR Effect: A Strategy for Overcoming the PEG Dilemma. *Adv. Drug Delivery Rev.* **2011**, *63*, 152−160.
(41) Tang, J.; Fu, H.; Kuang, Q.; Zhang, L.; Zhang, Q.; Liu, Y.; Ran, R.; Gao, H.; Zhang, Z.; He, Q. Liposomes Co-Modified with Cholesterol Anchored Cleavable PEG and Octaarginines for Tumor Targeted Drug Delivery. *J. Drug Targeting* **2014**, *22*, 313−326.
(42) Hatakeyama, H.; Akita, H.; Ito, E.; Hayashi, Y.; Oishi, M.; Nagasaki, Y.; Danev, R.; Nagayama, K.; Kaji, N.; Kikuchi, H.; Baba, Y.; Harashima, H. Systemic Delivery of siRNA to Tumors Using a Lipid Nanoparticle Containing a Tumor-Specific Cleavable PEG-lipid. *Biomaterials* **2011**, *32*, 4306−4316.
(43) Liu, J.; Liao, S.; Diop-Frimpong, B.; Chen, W.; Goel, S.; Naxerova, K.; Ancukiewicz, M.; Boucher, Y.; Jain, R. K.; Xu, L. TGF-beta Blockade Improves the Distribution and Efficacy of Therapeutics in Breast Carcinoma by Normalizing the Tumor Stroma. *Proc. Natl. Acad. Sci. U.S.A.* **2012**, *109*, 16618−16623.
(44) Lu, J.; Huang, Y.; Zhao, W.; Marquez, R. T.; Meng, X.; Li, J.; Gao, X.; Venkataramanan, R.; Wang, Z.; Li, S. PEG-derivatized Embelin as a Nanomicellar Carrier for Delivery of Paclitaxel to Breast and Prostate Cancers. *Biomaterials* **2013**, *34*, 1591−1600.
(45) Eldar-Boock, A.; Miller, K.; Sanchis, J.; Lupu, R.; Vicent, M. J.; Satchi-Fainaro, R. Integrin-Assisted Drug Delivery of Nano-Scaled Polymer Therapeutics Bearing Paclitaxel. *Biomaterials* **2011**, *32*, 3862−3874.
(46) Otake, A. H.; Mattar, A. L.; Freitas, H. C.; Machado, C. M.; Nonogaki, S.; Fujihara, C. K.; Zatz, R.; Chammas, R. Inhibition of Angiotensin II Receptor 1 Limits Tumor-Associated Angiogenesis and Attenuates Growth of Murine Melanoma. *Cancer Chemother. Pharmacol.* **2010**, *66*, 79−87.

DOI: 10.1021/acsami.5b01473
ACS Appl. Mater. Interfaces 2015, 7, 9691−9701